Dissection of synaptic excitability phenotypes by using a dominant-negative Shaker K^+ channel subunit

Timothy J. Mosca*†, Robert A. Carrillo*‡, Benjamin H. White§, and Haig Keshishian*¶

*Department of Molecular, Cellular, and Developmental Biology, Yale University, P.O. Box 208103, New Haven, CT 06520-8103; and ‡Department of Pharmacology, Yale University School of Medicine, P.O. Box 208066, New Haven, CT 06520-8066; §Laboratory of Molecular Biology, National Institute of Mental Health, National Institutes of Health, 36 Convent Drive, Building 36, Room 1B08, Bethesda, MD 20892-4034

Edited by Thomas C. Südhof, University of Texas Southwestern Medical Center, Dallas, TX, and approved January 18, 2005 (received for review August 20, 2004)

During nervous system development, synapses undergo morphological change as a function of electrical activity. In *Drosophila*, enhanced activity results in the expansion of larval neuromuscular junctions. We have examined whether these structural changes involve the pre- or postsynaptic partner by selectively enhancing electrical excitability with a Shaker dominant-negative (SDN) potassium channel subunit. We find that the SDN enhances neurotransmitter release when expressed in motoneurons, postsynaptic potential broadening when expressed in muscles and neurons, and selectively suppresses fast-inactivating, Shaker-mediated I_A currents in muscles. SDN expression also phenocopies the canonical behavioral phenotypes of the *Sh* mutation. At the neuromuscular junction, we find that activity-dependent changes in arbor size occur only when SDN is expressed presynaptically. This finding indicates that elevated postsynaptic membrane excitability is by itself insufficient to enhance presynaptic arbor growth. Such changes must minimally involve increased neuronal excitability.

activity | behavioral genetics | *Drosophila*

Electrical activity plays a prominent role in the development and plasticity of synapses (1–3). The glutamatergic neuromuscular junction (NMJ) of *Drosophila* is favorable for examining synaptogenesis and the role of electrical activity in synaptic growth and refinement (4, 5). In *Drosophila*, activity influences synaptic connectivity (6), size (7–9), and homeostasis (10, 11). Activity may also regulate retrograde signals that influence NMJ development (12–14). However, determining the relative contributions of pre- and postsynaptic excitability to synaptic development remains a significant challenge.

Addressing this problem requires molecular tools that selectively alter excitability on either side of the synapse. Early success in suppressing excitability has involved the targeted expression of modified ion channels or receptors (10, 15, 16). A promising approach for enhancing electrical activity involves the dominant-negative suppression of K^+ currents involved in membrane repolarization and excitability (17, 18).

The Shaker (Sh) type I_A K^+ current of *Drosophila* plays a key role in regulating membrane excitability of neurons and muscles (19, 20) and also influences the processing of graded potentials (21). *Sh* mutants have well characterized hyperactive behavioral and electrophysiological phenotypes (20, 22–24), making Sh a good candidate for dominant-negative suppression. Hyperexcitable *Sh* mutants, when combined with other K^+ channel mutants such as *ether-a-go-go*, also have enlarged larval NMJs (7–9). However, whether these structural changes arise from pre- or postsynaptic membrane hyperexcitability has remained unresolved, because the *Sh* mutation affects both neurons and muscle.

To dissect these changes, we have developed a Sh dominant-negative (SDN) transgene as a tool for targeted enhancement of electrical excitability. SDN effectively suppresses I_A, as demonstrated by voltage-clamp analysis of muscle, and also elevates spontaneous synaptic release events when expressed in neurons and broadens evoked postsynaptic potentials when expressed in muscles. The SDN also specifically phenocopies the principal adult and larval *Sh* behavioral phenotypes. At the NMJ, we observe that activity-dependent changes in neuronal morphology occur only when the SDN is presynaptically targeted. This finding provides strong evidence that activity-dependent arbor development minimally requires motoneuron hyperexcitability, and that enhanced muscle membrane excitability is insufficient to regulate motoneuron morphology through a retrograde signal.

Materials and Methods

Fly Stocks. All *Drosophila* strains were raised at 25°C on cornmeal-molasses food, with Canton S (CS) as wild type. UAS lines were expressed by using RU-486-inducible GeneSwitch (GS) GAL4 drivers (25) to drive expression panneuronally (elav-GS) or in all muscles (MHC-GS). The GS-GAL4 drivers allow for genetically identical control experiments, where the presence or absence of RU-486 is the only variable altered. Adult females were fed either 1.2 or 10 μg/ml RU-486 for 2 days before mating. Larvae were induced with either 1.2 or 10 μg/ml RU-486 in the food. For all experiments, negative controls were raised on plain medium lacking RU-486. Mutant lines included Sh^7, a Sh α-subunit truncation (26) that eliminates I_A (23); $maleless^{nap\text{-}ts1}$($mle^{nap\text{-}ts1}$), a mutation with reduced Na^+ conductance (27) that genetically suppresses *Sh* phenotypes (28, 29); and *ether-a-go-go* (eag^1), a K^+ channel subunit mutation that affects multiple K^+ currents (29–31). eag^1 virgins were crossed to male *T-SDN*^{204}; *elav-GS* or *T-SDN*^{204}; *MHC-GS* flies and male progeny selected.

Molecular Biology. SDN was generated from the EKO construct (32). The UAS-EKO$^+$ vector was cleaved at the end of the ORF and 3′ to the coding region for the S1 transmembrane helix. Two truncated UAS-EKO$^+$ constructs were generated, with or without an N-terminal GFP tag. The UAS-EKO$^+$ vector was religated with a 15-nt synthetic linker to introduce a UAG stop codon. The resultant UAS-SDN vectors encoded a predicted protein with the first 246 aa of the Sh K^+ channel, with residues 1–29 replaced by GFP. This protein resembles Sh1-246, a dominant-negative construct that suppresses Sh function *in vitro* (33, 34). Embryonic transformation was performed by using standard methods (35). Four viable SDN lines were obtained and mapped by using Vectorette PCR (36). The studies here used single copies of the viable T-SDN^{204} insert.

Imaging of Larvae. Third-instar larvae were dissected and fixed as described (37), mounted in glycerol, and imaged confocally

This paper was submitted directly (Track II) to the PNAS office.

Abbreviations: NMJ, neuromuscular junction; Sh, Shaker; SDN, Sh dominant-negative; EPSP, excitatory postsynaptic potential; GS, GeneSwitch; CS, Canton S.

†Present address: Department of Neurobiology, Harvard Medical School, 220 Longwood Avenue, Boston, MA 02115.

¶To whom correspondence should be addressed. E-mail: haig.keshishian@yale.edu.

(model no. 1024, Bio-Rad). To examine NMJ arbors, anti-horseradish peroxidase immunocytochemistry was performed as described (38).

Electrophysiology. Third-instar larvae were filleted as above to expose the body wall muscles. All miniature excitatory postsynaptic potential (EPSP) recordings were conducted on ventral longitudinal muscles 7, 6, 13, 12, and 4 in segments A2-A5 by using sharp microelectrodes (30–50 MΩ with 3M KCl) with a Dagan 8500 intracellular clamp (Dagan., Minneapolis), and PCLAMP 8.0 software (Axon Instruments). Physiological saline contained 140 mM NaCl , 5 mM KCl, 1 mM $CaCl_2$, 4 mM $NaHCO_3$, 6 mM $MgCl_2$, 5 mM TES–free acid, 5 mM trehalose, and 50 mM sucrose (pH 7.2). For frequency analysis, 10 1-s records were collected with 1 kHz low-pass filtering. Data were analyzed by using a one-way Student *t* test. Larval K^+ currents were examined by using a two electrode voltage clamp similar to above. Larvae were dissected in 0 mM Ca^{2+} physiological saline with 0.5 mM EGTA to eliminate the I_{CF} and I_{CS} calcium currents (32). The muscle was clamped at −80 mV and stepped to +30 mV in 10-mV increments. Currents were analyzed with CLAMPFIT 8.0. Current densities for both I_A and I_K were calculated by dividing peak current by muscle surface area, which is proportional to membrane capacitance (39). For all physiology experiments, *n* is expressed as the number of muscle fibers examined.

Nerve stimulations were performed by using a suction/stimulus microelectrode filled with physiological saline, attached immediately distal to muscle 13 on the SNb nerve branch. This stimulus location yields reliable single unit excitation of motoneurons, innervating the ventral longitudinal muscles, as previously demonstrated (37). EPSPs were obtained by using single-microelectrode impalements (20–30 MΩ with 3M KCl) under current clamp. Data were collected from muscle fibers 13 and 12 in segments A3 and A4 with stable resting membrane voltages at 60 ± 3 mV. Twenty EPSPs were collected per muscle. Mean EPSP amplitudes and half-widths (duration from 50% rise to 50% decay) for each synapse were determined by using CLAMPFIT 8.2. Data were analyzed by using a one-way Student *t* test.

Behavioral Assays. Adult flies were anesthetized with ether and examined for shaking and wing scissoring (40). To examine the behavior of isolated limbs, the legs of anesthetized flies were severed above the trochanter. To assess larval motility, crawling third-instar larvae were imaged at 2.5 frames per second on agar plates after acclimation. Speed was calculated on playback and analyzed by using a one-way Student *t* test.

Results

Molecular Characterization of SDN Transgenic Lines. We designed the SDN construct as a dominant-negative inhibitor of Sh channels to selectively enhance membrane excitability. SDN is a truncation of the wild-type Sh α-subunit after the first transmembrane helix (Fig. 1 *A* and *B*) and is modeled after an *in vitro*-characterized dominant-negative construct (33, 34, 41). It retains the T1 domain, a conserved N-terminal region necessary for subunit oligomerization (41) and axonal targeting (42). To monitor localization, the N-terminal fast inactivation domain (43) was replaced with GFP.

Single copies of SDN were expressed either panneuronally or panmuscularly. In either case, expression did not significantly reduce viability. Neuronal expression resulted in bright fluorescence throughout the central and peripheral neurons (Fig. 1*C*). Expression in larval muscles revealed uniform cytoplasmic GFP fluorescence (Fig. 1*D*). The subsynaptic reticulum, where Sh normally localizes (44), was not labeled, indicating that SDN does not accumulate at the NMJ as part of a Sh complex. Whereas some cytoplasmic fluorescence is likely due to proteolysis of nonfunctional SDN-Sh aggregates, it also suggests that SDN disrupts correct membrane targeting of Sh channels, perhaps by interfering with channel biogenesis (45).

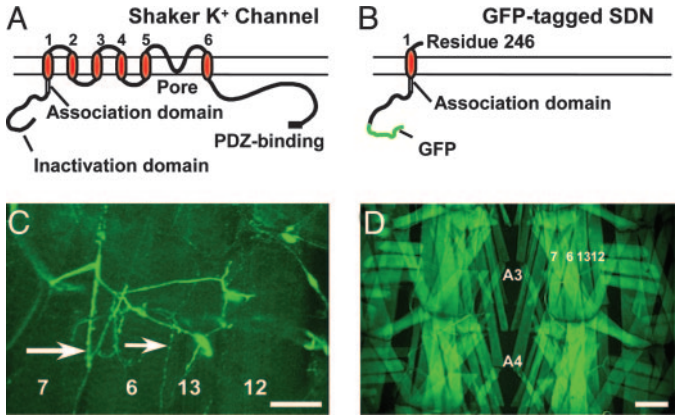

Fig. 1. Structure and expression of SDN. (*A*) Diagram of the full-length *Sh* α-subunit. Major structural features are labeled. (*B*) The truncated GFP-labeled SDN. (*C*) Confocal image of NMJ expression of SDN, driven by the *elav-GS* driver in a third-instar larva. Both Type I (large arrow) and type II (small arrow) presynaptic boutons are labeled. (Scale bar, 50 μm.) (*D*) Panmuscular expression of SDN by using the *MHC*-GS driver. Muscle fibers 7, 6, 13, and 12 are shown. (Scale bar, 100 μm.)

SDN Expression Eliminates the Fast-Inactivating A-Current, I_A. To determine the cellular effect of SDN expression, we examined larval muscle currents. SDN potently suppressed I_A, the Sh-mediated K^+ current. Control muscles in 0 mM Ca^{2+} normally exhibit two outward K^+ currents, I_A and I_K, (Fig. 2*A*) whereas *Sh* mutants exhibit only I_K (Fig. 2*B*, $n = 18$). In muscles expressing a single copy of SDN, I_A was attenuated 13-fold, with little effect on I_K (Fig. 2*C*, $n = 25$): current density was reduced to 0.085 ± 0.039 pA/μm^2 ($n = 25$) as compared with 1.141 ± 0.12 pA/μm^2 in wild-type (Fig. 2*D*, $n = 33$). SDN expression also had little effect on the kinetics of I_K. Peak I_K density showed no significant differences between wild-type, Sh^{7-}, or SDN-expressing muscles (Fig. 2*D*). There were also no significant differences in the activation voltage or peak current vs. voltage relationships for I_K (Fig. 2*E*). Our results are consistent with SDN functioning as a channel-specific dominant-negative inhibitor of Sh.

SDN Expression Enhances Neuronal Excitability. To study the effects of SDN on cellular excitability, we examined the frequency of spontaneous synaptic events at the NMJs (19, 29, 46) of panneuronally-driven SDN larvae. The frequency of spontaneous synaptic potentials (similar to vertebrate miniature end-plate potentials) is a widely used measure of synaptic function (11, 47–51) and scales with membrane excitability. Elevated spontaneous release is also characteristic of other activity mutants with reduced K^+ currents (46).

The frequency of spontaneous synaptic activity in larvae expressing a single copy of SDN panneuronally was nearly twice that of wild type, and similar to Sh^7 mutants (Fig. 3 *A* and *B*; SDN = 1.197 ± 0.152 Hz, $n = 39$; Sh^7 = 1.334 ± 0.138 Hz, $n = 57$; and CS = 0.613 ± 0.105 Hz, $n = 49$). For both SDN and Sh^7, the difference was statistically significant compared with wild type ($P < 0.001$). Moreover, synaptic activity was statistically indistinguishable between SDN and Sh^7 ($P > 0.5$), indicating that SDN closely phenocopies *Sh*. We also found that SDN's neural activity phenotype was suppressed by $mle^{nap\text{-}ts1}$, a classic genetic suppressor of *Sh*. Spontaneous activity was reduced to 0.485 ± 0.071 Hz ($n = 27$), a level indistinguishable from wild type ($P > 0.4$).

We also examined the effects of SDN on the amplitude and

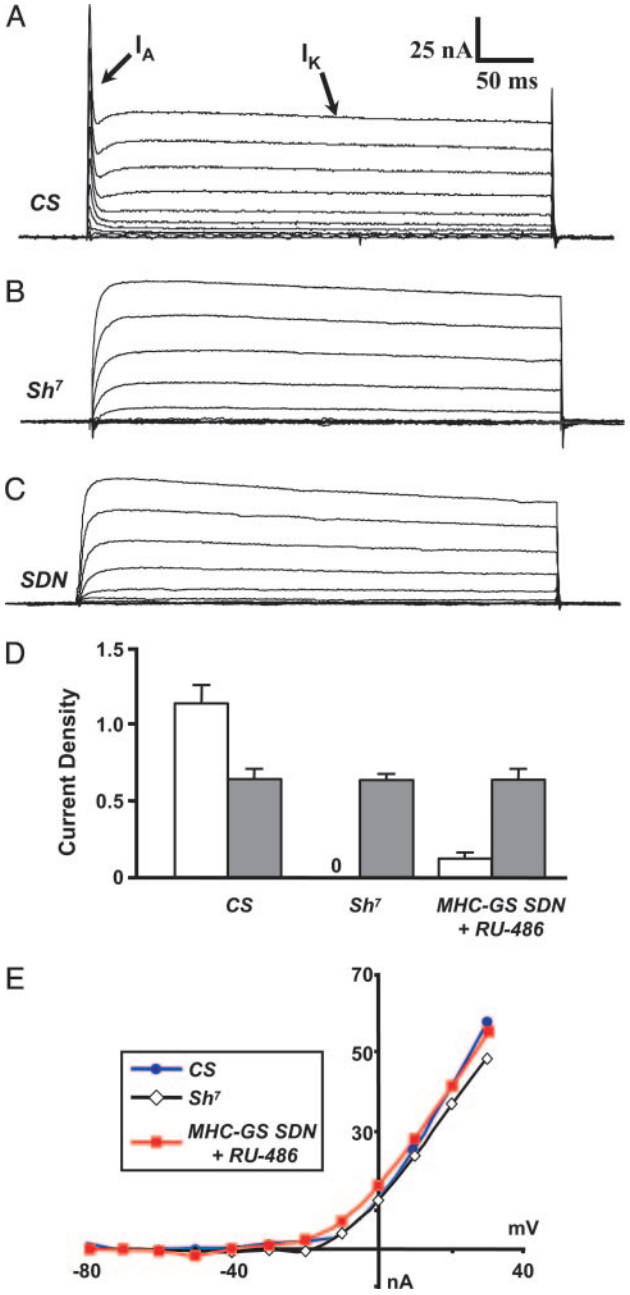

Fig. 2. SDN inhibits larval muscle I_A current. (*A*) Voltage clamp records of wild-type third-instar muscle showing both the transient Sh I_A and the delayed rectifier I_K currents. (*B*) In *Sh*^{7}, the transient I_A is absent, whereas I_K remains. (*C*) In larval muscles expressing SDN (*UAS-SDN*/+; *MHC-GS*/+). I_A is also absent, whereas I_K persists. (*D*) Peak current densities (at +30 mV) for I_A (white bars) and I_K (gray bars) in pA/μm^2. No I_A was observed for *Sh*^{7}. The peak I_K densities were, in each case, indistinguishable in amplitude. (*E*) Steady-state current–voltage relation (*I–V*) of I_K, showing no nonspecific effects of SDN.

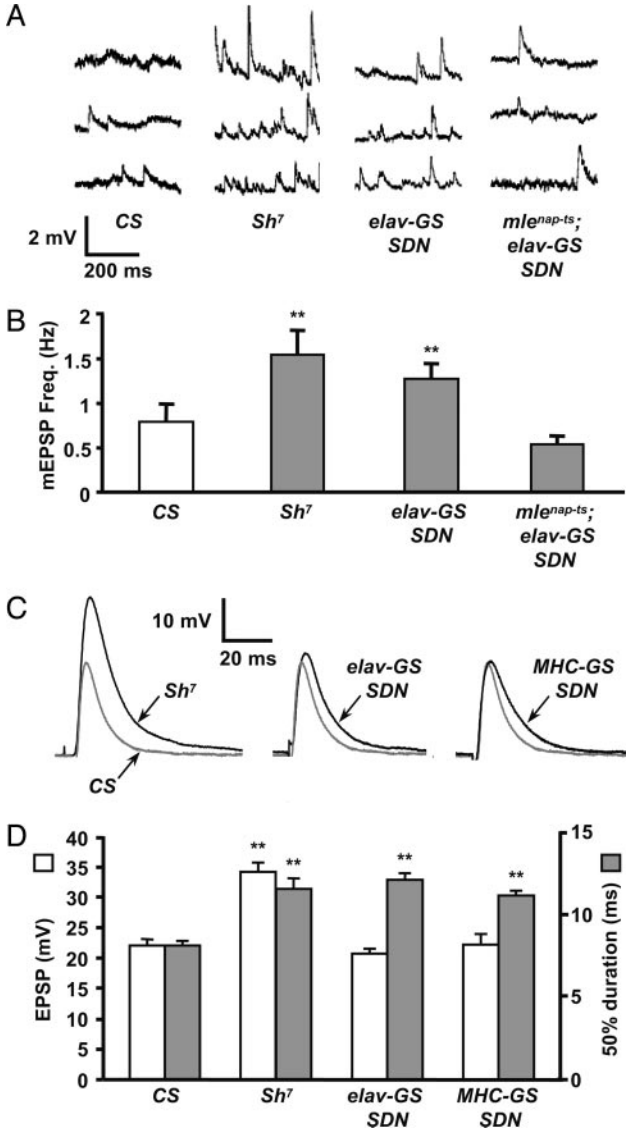

Fig. 3. SDN enhances both spontaneous and evoked EPSPs. (*A*) Spontaneous release events recorded in 1 mM Ca^{2+} from control (CS and *Sh*^{7}) and SDN-expressing larvae (*UAS-SDN*/+; *elav-GS*/+) and (*mle*$^{nap\text{-}ts1}$/*UAS-SDN*; *elav-GS*/+). The enhanced spontaneous event frequency observed in *Sh*^{7} larvae is phenocopied by neuronal SDN expression. The phenotype is suppressed by *mle*$^{nap\text{-}ts1}$. (*B*) Mean miniature EPSP frequencies are significantly increased in *Sh*^{7} (n = 56, $P < 0.001$ vs. CS) and in neuronal SDN-expressing larvae ($n = 38$, $P < 0.001$ vs. CS). *Sh*^{7} and neuronal SDN-expressing larvae are statistically indistinguishable ($P > 0.5$). Larvae with a *mle*$^{nap\text{-}ts1}$ suppression of SDN are indistinguishable from wild type ($n = 26$, $P > 0.4$). (*C*) Evoked EPSPs show significant broadening in both *Sh*^{7} and SDN-expressing motoneurons and muscles, compared with CS controls. Single motoneurons projecting to muscles 13 or 12 were excited by using stimulating electrode placements (37) in segments A3 and A4. The wild-type CS EPSP is gray for comparison with the mutant and SDN traces. (*D*) *Sh*^{7} shows a 62% increase in EPSP amplitude (white bars) and a 42% increase in PSP duration (gray bars) measured at 50% of peak amplitude ($n = 30$) compared with wild type ($n = 49$). Motoneuronal and muscle expression of SDN yielded a 49% ($n = 31$) and 37% ($n = 33$) increase in EPSP duration, respectively (**, $P < 0.001$ for all categories marked vs. CS). All data are mean ± SEM.

duration of evoked EPSPs. SDN was driven on either side of the NMJ, and EPSPs were compared with those observed in muscles of both wild-type and *Sh*^{7} larvae (Fig. 3 *C* and *D*). As previously reported (22, 26), *Sh* loss-of-function mutations, including *Sh*^{7}, result in substantially increased EPSP duration. We find that the EPSP half-width (measured at 50% of peak amplitude) was increased by 42% in *Sh*^{7} larvae (11.54 ± 0.60 ms, $n = 30$) compared with wild type (8.12 ± 0.28 ms, $n = 49$). This phenotype was dissected by driving expression of SDN on either side of the NMJ. Neuronal expression of SDN by using the elav-GS driver yielded a 49% increase in EPSP duration compared with wild type (12.10 ± 0.44 ms, $n = 31$), and muscle expression using the MHC-GS driver yielded a 37% increase (11.14 ± 0.31 ms, $n = 33$). All of these increases were highly

NEUROSCIENCE

Table 1. Adult behavioral phenotypes with *Sh* and SDN

Line or genotype	Leg	Wing	Cut leg
Canton S (wild type)	—	—	—
Sh^{14} (null allele)	Shake	Scissor	Shake
Sh^{7} (*DN* allele)	Shake	Scissor	Shake
*MHC-GS; SDN**	Shake	Scissor	Shake
MHC-GS; SDN	—	—	—
*elav-GS; SDN**	Shake	Scissor	Shake
elav-GS; SDN	—	—	—
$mle^{nap\text{-}ts1}$*; elav-GS; SDN**	—	—	—
$mle^{nap\text{-}ts1}$*; elav-GS; SDN*	—	—	—

—, No phenotype observed.
*RU-486-induced expression.

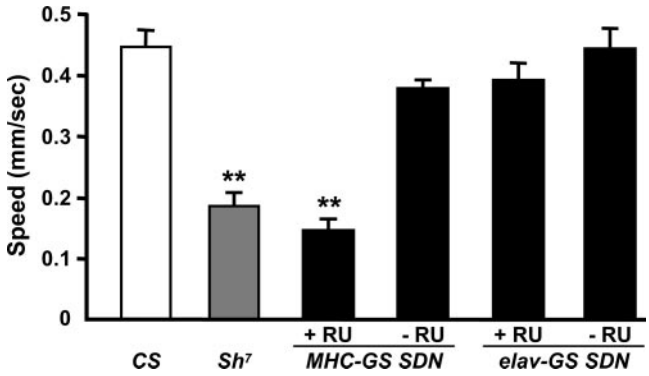

Fig. 4. Postsynaptic, but not presynaptic, SDN causes larval mobility defects. Average crawling speeds for control and SDN-expressing third-instar larvae. Speed decreases by 58% in Sh^7 larvae (n = 12 vs. CS) and by 68% in larvae expressing SDN panmuscularly (n = 9 vs. CS). Sh^7 and panmuscular SDN-expressing larvae were indistinguishable ($P > 0.2$). The motility defect is absent in uninduced MHC-GS SDN controls (n = 11, $P > 0.05$ vs. CS). When SDN is induced in neurons, no effect on crawling speed is observed (n = 11, $P > 0.1$ vs. CS or uninduced controls). For all controls, crawling speeds are not significantly different ($P > 0.5$). All data are mean ± SD. RU, RU-486. **, $P < 0.001$.

significant by t test ($P < 0.001$). Finally, we observed a significant increase in EPSP amplitude in Sh^7 compared with wild type (Sh^7: 34.1 ± 1.61 mV, n = 30; CS: 21.94 ± 1.14 mV, n = 49, $P \ll 0.001$), and no difference from wild-type amplitudes for either SDN transgenes when expressed singly on either side of the synapse (elav-GS: 20.7 ± 0.84 mV, n = 31; MHC-GS: 22.2 ± 1.75 mV, n = 33).

Cellular Locus of Action of Behavioral Phenotypes. Having demonstrated that SDN phenocopies the physiological phenotypes of *Sh*, we next examined whether SDN phenocopies the well known behavioral phenotypes of *Sh*, as a sensitive test for detecting nonspecific effects.

Adult phenotypes. Hyperexcitable mutants like *Sh* display abnormal leg shaking and wing scissoring in etherized adults (40, 52). We used SDN to dissect the cellular locus of this behavioral phenotype. Single copies of SDN induced both leg shaking and wing scissoring under ether anesthetization, regardless of whether it was expressed in neurons or muscle (Movie 1, which is published as supporting information on the PNAS web site). In all cases, noninduced etherized control or parental UAS/GAL4 flies were normal (Table 1). Abnormal leg shaking in hyperexcitable mutants persists in severed legs (40); this was also the case with neuronal or muscular SDN expression, indicating that hyperexcitability of either side of the NMJ is sufficient to cause the *Sh* behavioral phenotype (Table 1). Ether-induced leg shaking was also genetically suppressed by $mle^{nap\text{-}ts1}$ (Table 1). Thus, the SDN phenotypes resembled *Sh* mutants in both ether dependence and genetic suppression by $mle^{nap\text{-}ts1}$.

Larval locomotor phenotypes. Hyperexcitable mutant larvae exhibit decreased crawling speeds (53, 54). It has been proposed that hyperexcitability disrupts coordinated locomotor activity by reducing contraction efficiency (53). Both Sh^7 and panmuscular SDN-expressing third-instar larvae crawled more slowly than did controls (Fig. 4 and Movie 2, which is published as supporting information on the PNAS web site). Sh^7 larvae averaged 0.185 ± 0.079 mm/s (n = 12), and panmuscular SDN larvae averaged 0.144 ± 0.060 mm/s (n = 9). Both were significantly different from wild type (0.446 ± 0.028 mm/s, n = 12, $P < 0.001$) and indistinguishable from each other ($P > 0.4$). Noninduced larvae were also indistinguishable from their wild-type controls (n = 12, $P > 0.5$) (Movie 3, which is published as supporting information on the PNAS web site). By contrast, panneuronally expressed SDN had no effect on crawling speed (n = 12, $P > 0.2$ compared with CS). This finding indicates that locomotor *Sh* phenotypes result from muscle hyperexcitability and not from direct effects on the nervous system.

Presynaptic Hyperexcitability Is Necessary to Enhance Synaptic Arbor Growth. Having established that targeted expression of SDN effectively enhances excitability at the cellular and behavioral levels, we next addressed the role of excitability in NMJ development. SDN was expressed in either muscle fibers or neurons throughout development. As previous studies have shown that *Sh* synergizes with *eag* (7–9), we expressed SDN in either a wild-type or eag^1 background. Consistent with this idea, we observed a significant enlargement of motoneuron arbors only when SDN was expressed in the nervous system of eag^1 larvae, (Fig. 5 *A* and *B*). Induced eag^1/Y; *UAS-SDN/+*; *elav-GS/+* larvae averaged 88.2 ± 4.6 boutons on the ventral longitudinal muscles (Fig. 5*D*), a nearly twofold increase over controls (n = 9 larvae, $P < 0.001$, compared with CS). Similar enhancements were observed for the finer type II branches on muscles 12 and 13 (data not shown). Because bouton number and muscle size scale together (37, 55), we also examined muscle surface area relative to NMJ size (Fig. 5*D*). The average surface area of the ventral longitudinal muscle fibers in induced eag^1/Y; *UAS-SDN/+*; *elav-GS/+* larvae was indistinguishable from control larvae ($P > 0.2$), indicating that arbor expansion was due to causes other than changes in muscle size. In contrast, neuronal expression of SDN by itself did not alter the NMJ bouton number (Fig. 5*D*). Average bouton counts in induced *UAS-SDN/+*; *elav-GS/+* larvae were 50.5 ± 3.0 (n = 10) compared with 47.3 ± 2.8 for control larvae (n = 11 larvae, $P > 0.4$, compared with CS), with no significant difference in muscle fiber surface area (Fig. 5*D*, $P > 0.9$, compared with CS). The Sh^7 mutant also showed no significant alteration in bouton number (n = 9 larvae, $P > 0.1$, compared with CS). If the bouton counts of Sh^7 larvae are normalized to muscle surface area, the values are statistically indistinguishable from wild type (Fig. 5*D*). Thus, presynaptic expression of SDN phenocopies the previously described effects of *Sh* mutants on motoneurons arborization, including the requirement for *eag* to alter NMJ morphology.

To address whether Sh expression in the muscle is also required for changes in presynaptic arborization, we expressed SDN postsynaptically in eag^1 larvae and found no effect on NMJ morphology (Fig. 5*C*): the average bouton number was 38.7 ± 1.7 for induced eag^1/Y; *UAS-SDN/+*; *MHC-GS/+* larvae (n = 10 larvae, P = 0.01 vs. CS) and 47.3 ± 2.8 for CS larvae. Postsynaptic SDN expression in the absence of *eag* also had no effect (Fig. 5*D*, n = 8 larvae, $P > 0.05$ vs. CS). When muscle area is normalized, the differences between bouton counts become insignificant (Fig. 5*D*). The results indicate that increased mem-

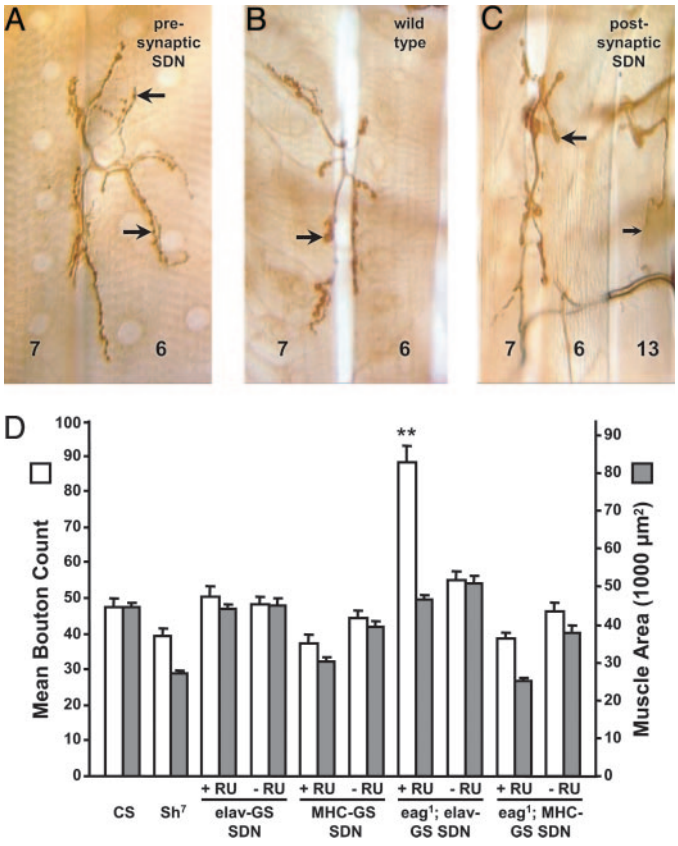

Fig. 5. Presynaptic SDN expression results in activity-dependent arbor enhancement. NMJs of larval muscles 6 and 7 in segment A2 are shown. Male larvae expressing SDN either pre- or postsynaptically, with or without an *eag*^{1} background, were scored. (*A*) Enlarged NMJs were observed only when SDN was driven neuronally in an *eag*^{1} background. (*B*) The type I boutons (large arrows) project more widely than in wild type. (*C*) By contrast, both type I (large arrow) and type II (small arrow) boutons exhibited wild-type morphology when SDN was expressed in the musculature in an *eag*^{1} background. (Scale bar, 25 μm.) (*D*) Mean bouton count (white bars) for muscles 6, 7, 12, and 13 of segment A4. Mean muscle areas are also shown (gray bars). No change in bouton number was observed for *Sh*^{7}, or for either neuronal or muscular SDN when expressed alone, without *eag*^{1}. By contrast, in the *eag*^{1} background, there is a marked increase in bouton number when SDN is expressed neuronally ($n = 9$ larvae, $P < 0.001$ vs. CS). The data pools Is and Ib boutons. This enhancement is not due to altered muscle size, because fiber width remains at wild-type levels ($P > 0.5$ vs. CS). By contrast, postsynaptic expression of SDN in an *eag*^{1} background had no effect on bouton count. Experimental and control values with and without RU486 induction are shown (+RU and −RU). All data are mean ± SEM. **, $P < 0.001$.

brane excitability of muscle is insufficient to influence presynaptic morphology through a retrograde action.

Discussion

The role of electrical excitability during synaptic development has been extensively examined (1–3, 56, 57), but manipulations targeted to specific sides of the synapse have been difficult. In *Drosophila*, there has been recent success using modified ion channels to suppress electrical excitability (15, 16). The overexpression of modified ion channels to enhance excitability has also been considered (17). In this paper, we truncated the Sh channel α-subunit to create an SDN construct to suppress I_A currents. *In vivo* tests using an inducible GAL4-UAS system (25) showed that SDN was readily expressed by neurons or muscles. Expression phenotypes resembled those of *Sh* mutations both physiologically and behaviorally. The data indicate that SDN functions *in vivo* as a dominant-negative suppressor of Sh, which is consistent with *in vitro* evidence (33, 34, 41). The observation that GFP-tagged SDN does not accumulate at postsynaptic membrane sites supports the view that truncated subunits disrupt channel biogenesis before surface membrane insertion (58).

Our results also show that the adult behavioral phenotypes of *Sh* are closely phenocopied by SDN expression in either neurons or muscles, and that SDN can be used to determine the cellular locus of action of *Sh* in generating these phenotypes. Hyperexcitability on either side of the adult NMJ is sufficient to generate an ether-dependent shaking phenotype. This finding was also true for isolated legs, where the only excitable cells are the muscles and the cut nerve ends. Therefore, the adult phenotype is likely a peripheral effect that arises from elevated synaptic release and muscle hyperexcitability, rather than a direct effect on central pattern generators (CPGs). The reduced larval locomotor phenotype associated with *Sh* occurred only when SDN was expressed in muscle. This finding again suggests that the locomotor phenotypes of *Sh* are due to muscle hyperexcitability, as opposed to a direct effect on CPGs. *Sh* mutations have also been shown to have minimal effects on other complex motor behaviors (59).

The physiological effects of SDN also mimicked the phenotypes of *Sh* mutations. We observed a significant increase in the frequency of miniature EPSPs after presynaptic expression of SDN, similar to that seen in *Sh* alleles, that could also be suppressed genetically by the *mle*$^{nap\text{-}ts1}$ mutation. This mutation reduces neuronal Na^+ channel density, supporting the view that SDN′s effects in the motoneuron are through elevated membrane excitability. We also observed a significant broadening of nerve-evoked EPSPs when SDN was expressed on either side of the NMJ, a characteristic phenotype of *Sh* mutations (24). This finding is likely due to action potential broadening when SDN is expressed presynaptically, through the loss of I_A in the motoneurons. The basis of EPSP broadening with muscle expression of SDN is also likely due to the loss of I_A at the postsynaptic density, where Sh channels normally localize (44). Finally, we note that it is necessary to have loss of I_A on both sides of the synapse to increase EPSP amplitude, as in *Sh*^{7}.

Electrical activity is essential for both the refinement and plasticity of neural circuits during development. Both hyper- and hypoexcitability alter the development of the *Drosophila* NMJ (6, 7, 9, 60). Electrical activity is also essential for regulating neuromuscular signaling through homeostatic feedback mechanisms that influence both presynaptic transmitter release and postsynaptic transmitter sensitivity (10, 11, 47). The effects of enhanced excitability on NMJ development have been investigated genetically, where *Sh* mutants exhibit expanded NMJs at room temperature in an *eag* background (7). However, because *Sh* mutants affect excitability on both sides of the NMJ, it has not been previously possible to determine whether this effect is pre- or postsynaptic (or both) in origin. Our results rule out a strictly postsynaptic locus of action: SDN expression fully mimics the effects of *Sh* mutants on NMJ arborization in its nature, severity, and genetic interaction with *eag* when expressed presynaptically (Fig. 5), but has no effect on arborization when expressed postsynaptically.

These results have interesting implications for the mechanisms governing activity-dependent NMJ growth. There is good evidence that retrograde transsynaptic signals strongly influence the size of the motoneuron terminal. Both the muscle-derived TGF-β growth factor Glass-bottom boat and the morphogen Wingless have been shown to function as transsynaptic regulators of NMJ growth (14, 61). The demonstration that muscle membrane excitability makes no direct contribution to NMJ growth rules out models in which muscle membrane depolarization alone determines the arbor-enhancing activity of such retrograde factors. Minimally, the motoneuron must be hyperexcit-

able for a structural change to occur. Taken together with evidence that the elevated expression of muscle glutamate receptors leads to significant NMJ expansion (62, 63), our results support a model where the well established retrograde control of motoneuron growth is influenced by synaptic receptor activation, rather than by muscle membrane depolarization.

In this model, current entering the muscle through glutamate receptors (including Ca^{2+}), as opposed to the voltage-activated current (probably through voltage-gated Ca^{2+} channels) is the critical first step for activity-dependent regulation of motoneuron growth. Presynaptic SDN expression elevates neurotransmitter release, and thus, postsynaptic receptor activation (Fig. 3), consequently resulting in enhanced arborization. By contrast, postsynaptic SDN expression only enhances membrane depolarization without directly altering the activation of muscle glutamate receptors (that are not voltage-gated) and thus has no effect on arborization. A prediction of this model is that the reciprocal manipulation, namely, selective suppression of muscle membrane excitability, should also have no effect on NMJ growth. This finding has been reported by Paradis *et al. (10)* by using directed expression of an inward rectifier K^+ channel, although this manipulation causes a compensatory elevation of presynaptic neurotransmitter release. Thus, manipulations that either increase (this study) or decrease (10) muscle membrane excitability do not directly affect motoneuron synaptic growth. Finally, we note that elevated presynaptic membrane excitability may potentiate the motoneuron's responsiveness to retrograde signals from the muscle, such as the growth factors essential for normal development of the synapse (49, 61). Examining whether SDN enhances or suppresses bone morphogenetic protein- or Wnt-mediated signal transduction will further resolve how synaptic growth is regulated by activity in this system.

The methods we present here provide a functional dissection of the role of electrical excitability at synapses. We anticipate that SDN will serve as a useful addition to the collection of activity modifying molecular constructs to resolve these and other problems in synaptic development and function.

We thank Thomas Osterwalder and Louise Nicholson for technical advice and assistance; Michael Gorczyca (University of Massachusetts Medical School, Worcester, MA) for the *Sh*^{7} fly stock; and Brett Berke, Greg Lnenicka, Michael Nitabach, Gary Yellen, and members of the Keshishian and Schwarz laboratories for helpful discussions and critical readings of the manuscript. This work was supported by National Science Foundation Grants IBN 0344595 and R01 NS31651 (to H.K.)

1. Goodman, C. S. & Shatz, C. J. (1993) *Cell* **72,** Suppl., 77–98.
2. Katz, L. C. & Shatz, C. J. (1996) *Science* **274,** 1133–1138.
3. Sanes, J. R. & Lichtman, J. W. (1999) *Annu. Rev. Neurosci.* **22,** 389–442.
4. Keshishian, H., Broadie, K., Chiba, A. & Bate, M. (1996) *Annu. Rev. Neurosci.* **19,** 545–575.
5. Gramates, L. S. & Budnik, V. (1999) *Int. Rev. Neurobiol.* **43,** 93–117.
6. Jarecki, J. & Keshishian, H. (1995) *J. Neurosci.* **15,** 8177–8190.
7. Budnik, V., Zhong, Y. & Wu, C. F. (1990) *J. Neurosci.* **10,** 3754–3768.
8. Zhong, Y., Budnik, V. & Wu, C. F. (1992) *J. Neurosci.* **12,** 644–651.
9. Zhong, Y. & Wu, C. F. (2004) *J. Neurosci.* **24,** 1439–1445.
10. Paradis, S., Sweeney, S. T. & Davis, G. W. (2001) *Neuron* **30,** 737–749.
11. Davis, G. W., DiAntonio, A., Petersen, S. A. & Goodman, C. S. (1998) *Neuron* **20,** 305–315.
12. Koh, Y. H., Gramates, L. S. & Budnik, V. (2000) *Microsc. Res. Tech.* **49,** 14–25.
13. Fitzsimonds, R. M. & Poo, M. M. (1998) *Physiol. Rev.* **78,** 143–170.
14. Keshishian, H. & Kim, Y.-S. (2004) *Trends Neurosci.* **27,** 143–147.
15. White, B., Osterwalder, T. & Keshishian, H. (2001) *Curr. Biol.* **11,** R1041–R1053.
16. Nitabach, M. N., Blau, J. & Holmes, T. C. (2002) *Cell* **109,** 485–495.
17. Broughton, S. J., Kitamoto, T. & Greenspan, R. J. (2004) *Curr. Biol.* **14,** 538–547.
18. Nerbonne, J. M., Nichols, C. G., Schwarz, T. L. & Escande, D. (2001) *Circ. Res.* **89,** 944–956.
19. Jan, Y. N., Jan, L. Y. & Dennis, M. J. (1977) *Proc. R. Soc. London Ser. B* **198,** 87–108.
20. Salkoff, L. & Wyman, R. (1981) *Science* **212,** 461–463.
21. Niven, J. E., Vahasoyrinki, M., Kauranen, M., Hardie, R. C., Juusola, M. & Weckstrom, M. (2003) *Nature* **421,** 630–634.
22. Tanouye, M. A. & Ferrus, A. (1985) *J. Neurogenet.* **2,** 253–271.
23. Wu, C. F. & Haugland, F. N. (1985) *J. Neurosci.* **5,** 2626–2640.
24. Haugland, F. N. & Wu, C. F. (1990) *J. Neurosci.* **10,** 1357–1371.
25. Osterwalder, T., Yoon, K. S., White, B. H. & Keshishian, H. (2001) *Proc. Natl. Acad. Sci. USA* **98,** 12596–12601.
26. Gisselmann, G., Sewing, S., Madsen, B. W., Mallart, A., Angaut-Petit, D., Muller-Holtkamp, F., Ferrus, A. & Pongs, O. (1989) *EMBO J.* **8,** 2359–2364.
27. Wu, C. F., Ganetzky, B., Jan, L. Y. & Jan, Y. N. (1978) *Proc. Natl. Acad. Sci. USA* **75,** 4047–4051.
28. Reenan, R. A., Hanrahan, C. J. & Barry, G. (2000) *Neuron* **25,** 139–149.
29. Ganetzky, B. & Wu, C. F. (1982) *J. Neurophysiol.* **47,** 501–514.
30. Zhong, Y. & Wu, C. F. (1991) *Science* **252,** 1562–1564.
31. Zhong, Y. & Wu, C. F. (1993) *J. Neurosci.* **13,** 4669–4679.
32. White, B. H., Osterwalder, T. P., Yoon, K. S., Joiner, W. J., Whim, M. D., Kaczmarek, L. K. & Keshishian, H. (2001) *Neuron* **31,** 699–711.
33. Tang, C. Y., Schulteis, C. T., Jimenez, R. M. & Papazian, D. M. (1998) *Biophys. J.* **75,** 1263–1270.
34. Schulteis, C. T., Nagaya, N. & Papazian, D. M. (1998) *J. Biol. Chem.* **273,** 26210–26217.
35. Rubin, G. M. & Spradling, A. C. (1982) *Science* **218,** 348–353.
36. Eggert, H., Bergemann, K. & Saumweber, H. (1998) *Genetics* **149,** 1427–1434.
37. Lnenicka, G. A. & Keshishian, H. (2000) *J. Neurobiol.* **43,** 186–197.
38. Johansen, J., Halpern, M. E., Johansen, K. M. & Keshishian, H. (1989) *J. Neurosci.* **9,** 710–725.
39. Jan, L. Y. & Jan, Y. N. (1976) *J. Physiol.* **262,** 189–214.
40. Kaplan, W. D. & Trout, W. E. (1969) *Genetics* **61,** 399–409.
41. Li, M., Jan, Y. N. & Jan, L. Y. (1992) *Science* **257,** 1225–1230.
42. Gu, C., Jan, Y. N. & Jan, L. Y. (2003) *Science* **301,** 646–649.
43. Hoshi, T., Zagotta, W. N. & Aldrich, R. W. (1990) *Science* **250,** 533–538.
44. Tejedor, F. J., Bokhari, A., Rogero, O., Gorczyca, M., Zhang, J., Kim, E., Sheng, M. & Budnik, V. (1997) *J. Neurosci.* **17,** 152–159.
45. Papazian, D. M. (1999) *Neuron* **23,** 7–10.
46. Ganetzky, B. & Wu, C. F. (1983) *J. Neurogenet.* **1,** 17–28.
47. DiAntonio, A., Petersen, S. A., Heckmann, M. & Goodman, C. S. (1999) *J. Neurosci.* **19,** 3023–3032.
48. Aberle, H., Haghighi, A. P., Fetter, R. D., McCabe, B. D., Magalhaes, T. R. & Goodman, C. S. (2002) *Neuron* **33,** 545–558.
49. McCabe, B. D., Marques, G., Haghighi, A. P., Fetter, R. D., Crotty, M. L., Haerry, T. E., Goodman, C. S. & O'Connor, M. B. (2003) *Neuron* **39,** 241–254.
50. Davis, G. W., Schuster, C. M. & Goodman, C. S. (1996) *Neuron* **17,** 669–679.
51. Yoshihara, M., Suzuki, K. & Kidokoro, Y. (2000) *J. Neurosci.* **20,** 8315–8322.
52. Wang, J. W., Humphreys, J. M., Phillips, J. P., Hilliker, A. J. & Wu, C. F. (2000) *J. Neurosci.* **20,** 5958–5964.
53. Wang, J. W., Sylwester, A. W., Reed, D., Wu, D. A., Soll, D. R. & Wu, C. F. (1997) *J. Neurogenet.* **11,** 231–254.
54. Wang, J. W., Soll, D. R. & Wu, C. F. (2002) *J. Neurogenet.* **16,** 45–63.
55. Schuster, C. M., Davis, G. W., Fetter, R. D. & Goodman, C. S. (1996) *Neuron* **17,** 641–654.
56. Aamodt, S. M. & Constantine-Paton, M. (1999) *Adv. Neurol.* **79,** 133–144.
57. Goda, Y. & Davis, G. W. (2003) *Neuron* **40,** 243–264.
58. Page, K. M., Heblich, F., Davies, A., Butcher, A. J., Leroy, J., Bertaso, F., Pratt, W. S. & Dolphin, A. C. (2004) *J. Neurosci.* **24,** 5400–5409.
59. Phillis, R. W., Bramlage, A. T., Wotus, C., Whittaker, A., Gramates, L. S., Seppala, D., Farahanchi, F., Caruccio, P. & Murphey, R. K. (1993) *Genetics* **133,** 581–592.
60. Lnenicka, G. A., Spencer, G. M. & Keshishian, H. (2003) *J. Neurobiol.* **54,** 337–345.
61. Packard, M., Koo, E. S., Gorczyca, M., Sharpe, J., Cumberledge, S. & Budnik, V. (2002) *Cell* **111,** 319–330.
62. Sigrist, S. J., Thiel, P. R., Reiff, D. F. & Schuster, C. M. (2002) *J. Neurosci.* **22,** 7362–7372.
63. Sigrist, S. J., Reiff, D. F., Thiel, P. R., Steinert, J. R. & Schuster, C. M. (2003) *J. Neurosci.* **23,** 6546–6556.